Communication

Shape-Controlled Synthesis of Manganese Oxide Octahedral Molecular Sieve Three-Dimensional Nanostructures

Jikang Yuan, Wei-Na Li, Sinue Gomez, and Steven L. Suib

J. Am. Chem. Soc., **2005**, 127 (41), 14184-14185• DOI: 10.1021/ja053463j • Publication Date (Web): 24 September 2005

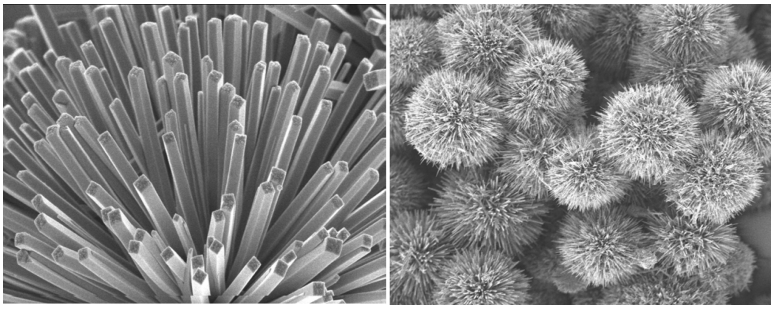

J|A|C|S
COMMUNICATIONS

Published on Web 09/24/2005

Shape-Controlled Synthesis of Manganese Oxide Octahedral Molecular Sieve Three-Dimensional Nanostructures

Jikang Yuan,[†] Wei-Na Li,[†] Sinue Gomez,[†] and Steven L. Suib*[,†,‡,||]

Department of Chemistry, Department of Chemical Engineering, and Institute of Materials Science, Unit 3060, 55 North Eagleville Road, University of Connecticut, Storrs, Connecticut 06269-3060

Received May 27, 2005; E-mail: steven.suib@uconn.edu

Direct architecture of complex nanostructures is desirable and still remains a challenge in areas of materials science.[1] Due to their size- and shape-dependent electronic and optical properties, much effort has been made to control morphologies of transition metal oxide nanoparticles and to organize them into complicated 3D structures using templates.[2] In particular, manganese oxides have attracted much attention because they have extensive applications in many chemical processes due to their porous structures, acidity, ion-exchange, separation, catalysis, and energy storage in secondary batteries.[3] Using organic templates, such as trimethylamine (TMA), manganese oxides have been successfully organized into macroscopic rings and helices via sol−gel processes.[4] However, the methods mentioned above all need further purification, so impurities will be introduced. Subsequent procedures are needed to obtain pure products. Thus, facile and organic template-free methods are highly desired for synthesis of manganese oxide nanoparticles with complex 3D structures.

Manganese oxide octahedral molecular sieves (OMS) are a class of microporous transition metallic oxides with various kinds of tunnel structures that can be synthesized via controlling synthetic conditions, such as temperature, concentration, pH, and cations.[5] Manganese oxide molecular sieves are semiconducting mixed-valence catalysts that have distinct advantages over aluminosilicate molecular sieve materials for applications in catalysis due to the mixed-valence character.[6] In particular, cryptomelane-type manganese oxide (OMS-2) nanoparticles can be easily prepared via reflux at lower temperatures.[7] However, synthesis of OMS-2 nanoparticles with uniform shapes and organization of them into ordered 3D nanostructures is still a challenge and requires precise control over synthetic parameters, such as temperatures, acidities, and redox potentials. Herein, we report the preparation of uniform OMS-2 3D dendritic and spherical nanostructures under mild hydrothermal conditions.

In a typical synthesis, 12 mmol of $MnSO_4 \cdot H_2O$ and 4 mmol of $K_2Cr_2O_7$ were mixed with 15 mL of deionized (DI) water, followed by an addition of 1.542 mL of H_2SO_4 to form a clear solution, which was then transferred to a 23 mL Teflon-lined autoclave. The autoclave was sealed and heated in an oven at 120 °C for 12 h. The resulting black slurry was rinsed with DI water several times to remove soluble impurities. The product was dried in an oven at 120 °C for 4 h. The whole process can be easily adjusted to prepare manganese oxide with different 3D nanostructures by simply increasing temperature to 180 °C while keeping other conditions unchanged. Further characterization methods include X-ray diffraction (XRD), scanning electronic microscopy (SEM), and transmission electron microscopy (TEM).

X-ray powder diffraction (XRD) analyses of the products were carried out on a Scintag X-ray diffractometer with Cu Kα radiation ($\lambda = 0.15406$ nm) operating at 40 mA and 45 kV. All observed peaks can be indexed to a pure tetragonal cryptomelane (OMS-2) phase with lattice parameters $a = b = 9.82$ Å and $c = 2.85$ Å. The sharp peaks of Figure 1A imply larger crystallinity. This is in contrast to that of B, in which OMS-2 nanoparticles were synthesized at higher temperature (180 °C). The peaks of B are broader, implying smaller crystallinity. Notable preferred orientations were also observed for (220), (400), (330), (420), and (510) planes of OMS-2 synthesized at lower temperature (120 °C).

The morphologies of as-synthesized microporous OMS-2 were obtained by field emission scanning electron microscopy (FESEM). Figure 2 reveals that, at 120 °C, the nanoparticles can be self-organized into dendritic nanostructures with diameters of each cluster of about 4 μm. The nanocluster arrays are composed of uniform tetragonal prism nanorods with square cross-sections. The length of each individual nanorod is about 2 μm. The length of each side of the square is about 200 nm. The nanorods of each cluster originate from the same core particles. However, increasing temperature (180 °C) leads to formation of dandelion-like microspheres with diameters of about 5 μm. The microspheres are composed of OMS-2 nanoneedles with sharp tips, as shown in Figure 3. The OMS-2 nanoneedles have diameters of about 40 nm and lengths of about 2.5 μm.

The products were further characterized by transmission electron microscopy (TEM), as shown in Figure 4. Electron diffraction patterns of individual nanorods and the clear lattice fringes clearly show that the OMS-2 nanoscale tetragonal prisms are single crystalline. The width of two neighboring lattice fringes corresponds to the (200) planes. The width of 6.67 Å from neighboring fringes of individual nanowires corresponds to (110) planes of cryptomelane-type OMS-2. Further investigation of electron diffraction (ED) of individual nanoscale tetragonal prisms shows that the growth direction of each individual nanorod is along [001] with growth axis planes of (002). Figure 4 C,D also shows single-crystalline OMS-2 nanowires from OMS-2 mesoscopic spheres with diameters of about 40 nm and *d* spacings of 6.67 Å that correspond to (110) planes.

Formation of uniform and monodisperse nanostructures requires precise control over nucleation and growth processes.[8] The redox potential of $Cr_2O_7^{2-}/Cr^{3+}$ (1.33 V) is just a little bit higher than that of Mn^{4+}/Mn^{2+} (1.23 V), so that the reaction is mild and slow, resulting in formation of well-organized OMS-2 complex morphologies. Temperature also plays an important role in controlling OMS-2 morphologies by means of controlling nucleation processes. Increasing temperature facilitates homogeneous nucleation, resulting in formation of OMS-2 microspheres. Interfacial tension and hydrophilic surfaces of OMS-2 nanocrystals may be the driving forces for the formation of dendritic and spherical OMS-2 nanostructures. By means of using other dichromate and chromate salts

[†] Institute of Materials Science.
[‡] Department of Chemistry.
[||] Department of Chemical Engineering.

10.1021/ja053463j CCC: $30.25

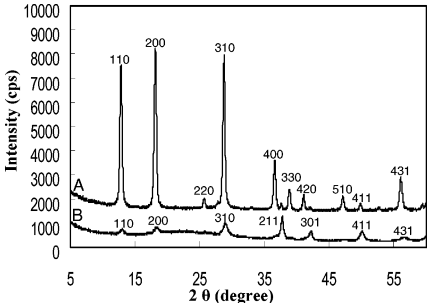

Figure 1. Representative XRD patterns of as-synthesized OMS-2 3D nanostructures obtained by hydrothermal treatment of manganese sulfate and potassium dichromate under acid conditions. (A) OMS-2 synthesized at 120 °C; (B) OMS-2 obtained at 180 °C. (The peaks of A and B can all be indexed to pure cryptomelane-type OMS-2 phase.)

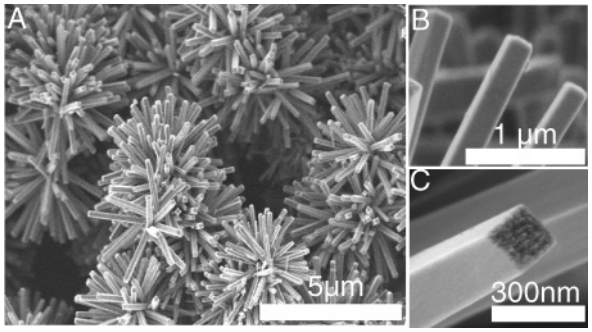

Figure 2. SEM images of OMS-2 dendritic clusters composed of nanotetragonal prisms with square cross-section obtained from hydrothermal reaction at 120 °C, 12 h. (A−C) Detailed views of the same cluster with higher magnifications.

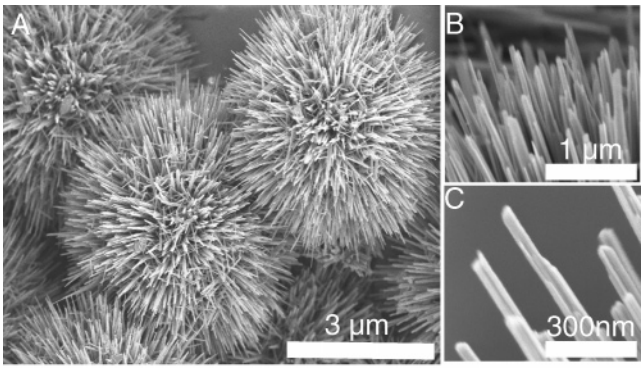

Figure 3. (A) FESEM images of as-synthesized OMS-2 microspheres obtained at 180 °C, 12 h. (B, C) Images of a selected microsphere with higher magnifications.

as starting materials, we have successfully prepared some complex 3D OMS nanostructures with various tunnel structures and morphologies.

In summary, we successfully synthesized novel OMS-2 nanostructures under mild and organic template-free conditions. The shape evolution of OMS-2 can be performed via simply varying temperature. The hierarchically ordered nanoscale architectures of

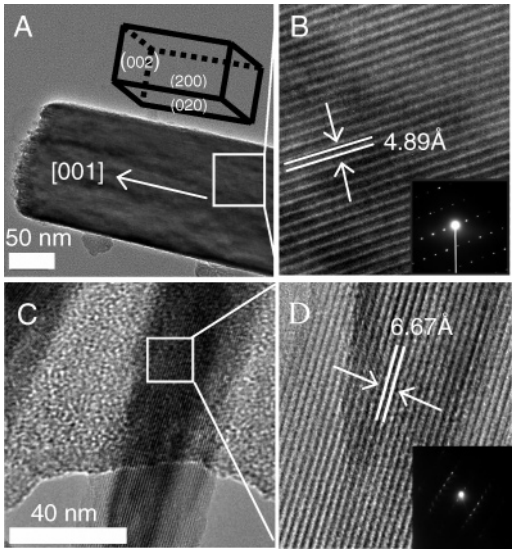

Figure 4. Selected area TEM (SATEM) images of individual OMS-2 nanorods and nanowires. (A and B) TEM images of an individual nanotetragonal prism. (C and D) SATEM of an individual nanowire from a microsphere. Insets of B and D: electron diffraction patterns of A and C, respectively.

OMS-2 originated from primary microporous structures of cryptomelane-type manganese oxides, secondary structures of uniform nanoparticles, and tertiary architectures of microscopic arrays. These OMS-2 nanoparticles with specific structures may find potential applications in sensors, catalysis, biomarkers, microelectronics, and energy storage.

Acknowledgment. This project is funded by the Geosciences and Biosciences Division of the Office of Basic Energy Sciences, Office of Science, U.S. Department of Energy. We also acknowledge Mr. Jim Romanow and Steve Daniels for providing access to TEM and FESEM facilities in the Department of Physiology and Neurobiology Department of UConn, Mark Aidow for use of the JEOL 2010 TEM in the Institute of Materials, UConn, as well as Dr. Frank Galasso for helpful discussions.

References

(1) (a) Huang, Y.; Duan, X.; Wei, Q.; Leiber, M. C. *Science* **2001**, *291*, 630−633. (b) Alivisatos, A. P. *Science* **1996**, *271*, 933−937.
(2) (a) Sun, Y.; Xia, Y. *Science* **2002**, *298*, 2176−2179. (b) Tian, R. Z.; Voigt, A. J.; Liu, J.; Mckenzie, B.; Mcdermott, J. M.; Rodriguez, A. M.; Konishi, H.; Xu, H. *Nat. Mater.* **2003**, *2*, 821−826. (c) Yu, D.; Yam W. V. *J. Am. Chem. Soc.* **2004**, *126*, 13200−13201.
(3) (a) Chabre, Y.; Pannetier, J. *Prog. Solid State Chem.* **1995**, *23*, 1−130. (b) Shen, Y. F.; Zerger, P. R.; DeGuzman, N. R.; Suib, L. S.; McCurdy, L.; Potter, I. D.; O'Young, C. L. *Science* **1993**, *260*, 511−515. (c) Paik, Y.; Osegovic, P. J.; Wang, F.; Bowden, W.; Grey, P. C. *J. Am Chem. Soc.* **2001**, *123*, 9367−9377.
(4) Giraldo, O.; Marquez, M.; Brock, L. S.; Suib, L. S.; Hillhouse, H.; Tsapatsis, M. *J. Am. Chem. Soc.* **2000**, *122*, 12158−12163.
(5) (a) Turner, S.; Buseck, R. P. *Science* **1979**, *203*, 456−458. (b) Zhang, I.; Burnham, W. C. *Am. Mineral.* **1994**, *79*, 168−174.
(6) Son, Y.; Makawana, D. V.; Howell, R. A.; Suib, L. S. *Angew. Chem., Int. Ed.* **2001**, *40*, 4280−4283.
(7) McKenzie, R. M. *Miner. Magn. J. Miner. Soc.* **1971**, *38*, 493−502.
(8) Xia, Y.; Yang, P.; Sun, Y.; Wu, Y.; Mayers, B. G.; Yin, Y.; Kim, F.; Yan, H. *Adv. Mater.* **2003**, *15*, 353−389.

JA053463J